RESEARCH ARTICLE

Key Technology of Mixed Matching Circuit for Miniaturizing Dual-Band Antenna

DAOHENG ZHU [1], DAIAN LU[2], XIAOKUN YANG[3], AND ZHIQIANG LI[1]

[1]College of Electronics and Information Engineering, Guangdong Ocean University, Zhanjiang 524088, China
[2]China Communications Service Guizhou Company Ltd., Guiyang 550005, China
[3]College of Big Data and Information Engineering, Guizhou University, Guiyang 550025, China

Corresponding author: Zhiqiang Li (qiangzl1974@163.com)

ABSTRACT A mixed matching circuit for miniaturizing dual-band antenna is introduced and verified in this study. Two L-shaped matching circuit for miniaturization are cascaded to interpret the theory of operation in accordance with the dual-band allocations on the Smith chart. A matching circuit equation is deduced based on a bidirectional matching track from a certain position to the origin point on the Smith chart. Furthermore, a dual-band antenna is taken as an example to illustrate the performance of the novel matching approach for miniaturization. The occupation of a dual-band antenna can be reduced by a quarter at the simultaneous operational frequencies of 2.4 and 5.8 GHz. Lastly, a dual-band planar inverted-F antenna (PIFA) is developed and examined. The experimental results are well consistent with those in the simulator.

INDEX TERMS Dual-band antenna, PIFA, the Simth Chart, matching circuit.

I. INTRODUCTION

Radio Frequency (RF) matching circuit can make the mismatching loads work at arbitrary frequencies with maximum efficiency. Numerous technologies based on the matching circuit have been reported. For instance, multi-band filtering techniques have been reported to deal with the signal noise, whereas it cannot be applied extensively due to the disadvantages of massive load loss compared with normal filter [1]–[3]. Subsequently, several excellent matching blocks based on parameter extraction for two complex impedances were demonstrated using the Smith chart [4], [5]. Although sufficient theoretical results regarding the lumped LC resonant circuit have been obtained, few applications based on them were illustrated except for load matching [6].

Small mobile devices have become popular among the young for their portable property and multifarious types. Moreover, tech giants like Samsung, Motorola and Huawei announced novel foldable mobile devices attracting much attentions, one by one [7], [8]. Keeping up with their paces, there will be more accessories (e.g., foldable material, screen

and special antenna designed for foldable devices). Foldable and multi-band antenna has been proposed for such applications [9]–[11]. Conformal antennas featuring easy bending and low profile was also under consideration for foldable electronic devices, whereas they have not been applied thus far for their bulky volume will destroy the aesthetic of appearance [12], [13]. Accordingly, the relative researches of miniaturization became urgent issues to be dealt with. Especially, a key part for miniaturization was antenna, usually designer miniaturize the antenna by designing the meandering line, which will cost lots of time on optimization for a desired result. Considering the antenna as a load with different impedance, the matching circuit can efficiently reduce the occupation of antenna. Miniaturized antenna based on matching circuits became a potential candidate for low-cost mobile devices [14], [15]. In previous research, miniaturized antennas have been already applied in mobile devices, the meander-line antenna for wireless network was proposed and its experimental results have verified the scheme [16]. Reference [17] presented a complex miniaturized quad-band antenna for tablet computers, whereas its −10 dB (less than −6 dB) bands in two low frequencies is too weak to capture signals in principle. Reference [18] developed a small slot
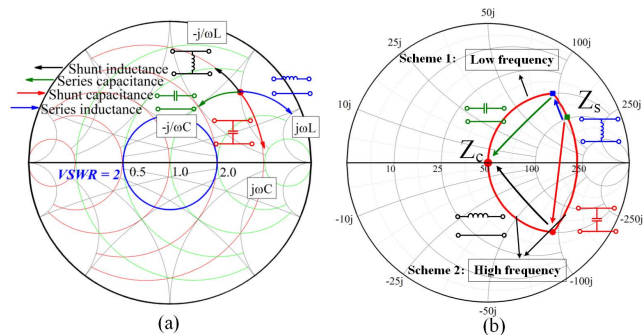
FIGURE 1. Two foldable types. (a) vertical folding model, (b) horizontal folding mode.

FIGURE 2. Geometry of the PIFA with detailed parameters.

loop antenna with a simple matching circuit and verified its capacity on laptop, which has also laid a basis for the assumption of a miniaturized dual-band antenna. Reference [19] developed a dual-band monopole antenna comprising the Worldwide Interoperability for Microwave Access (WiMAX) and WLAN bands, and the antenna exhibits approximately omnidirectional radiation characteristics with high gain and efficiency. Reference [20] proposed a wearable all-textile metasurface antenna (MSA) for 5 GHz wireless body area network (WBAN) applications. The researchers confirmed that the MSA is stable and secure through experiments, and the MSA is suitable used for a wide variety of wearable applications in the 5 GHz WBAN.

A multi-band PIFA usually comprises at least three meandering stubs affecting the reflection coefficient in dual bands [21], [22]. The proposed miniaturized PIFA was printed on a 0.4 mm FR4 substrate with permittivity of 4.4 and loss tangent of 0.02, which can be mounted in the left-up corner of the mock-up for vertical and horizontal folding, corresponding to the representations of Huawei's high-end vertical folding production and Samsung's horizontal folding production. In principle, the occupation of the RF component can be tailored as small as possible by cascading a matched circuit [23]. However, a 25% off for size will be illustrated to verify the operation of the proposed dual-band matching scheme due to the performance of radiated pattern, sensitive resonance and actual requirement in exercise.

The residual section of this study is organized as following: the miniaturized theory based on impedance matching principle is introduced in section II. Besides, a PIFA is taken as an example to illustrate the flow of miniaturization. The reduction of a quarter on occupation is achieved compared with the normal PIFA who resonates at 2.4 and 5.8Gz. The equivalent parameter extraction and the way to connect two matching circuit are presented in section III. Lastly, a prototype will be developed and examined to conduct a comparison between experiment and simulation. Both results are well consistent with each other.

II. MATCHING SCHEME
The respective component exhibits individual property of shifting phase which can be concluded by several tracks on
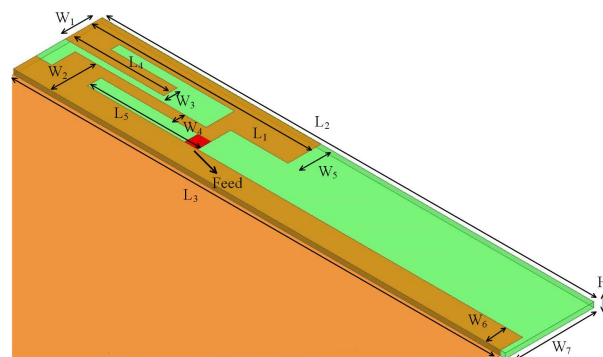
the Smith chart, as presented in Fig. 1(a). They are considered to move along a circle during the change of their values. In theory, there will be infinite tracks from a certain point to the center of the Smith chart meaning lots of schemes to match a RF system [24]. However, only the least elements will lead to the minimum loss. Moreover, special tracks are suitable for different frequencies. In low frequencies, parallel inductance and series capacitance will work in accordance with the track of top semicircle in Fig. 1(b). In contrast, series inductance and parallel capacitance will work in high frequency according to the bottom semicircle. An equation for dual-band matching circuit is deduced and simplified according to the two bidirectional tracks to the center, a series of equations are as following:

$$Z_c = \begin{cases} Z_s + (-j/\omega_1 L) + (-j/\omega_1 C)(1.a) \\ Z_s + j\omega_2 L + j\omega_2 C (1.b) \end{cases} \quad \omega_1 < \omega_2$$

$$\tag{1}$$

$$Z_c = Z_s + (-j/\omega L_1) + (-j/\omega C_1) + j\omega L_2 + j\omega C_2 \tag{2}$$

$$Z_c = Z_s + j[(-1)(L_1^{-1} + C_1^{-1})\omega^{-1} + (L_2 + C_2)\omega] \tag{3}$$

where Z_s denotes the impedance extracted from miniaturized antenna. Notably, two or more Z_s can be simultaneously found on the Smith chart because of different operational frequency ω. L and C are the inductance and capacitance of lumped circuit. Thus, Eq. (1. a) and (1. b) respectively denote two matching states at the frequency of ω_1 and ω_2. Eq. (2) for dual-band situation can be deduced by combining Eq. (1. a) and (1. b) and can be further simplified to obtain Eq. (3). It can be clearly stated that the larger the difference between ω_1 and ω_2, the better the working performance of the equation. Accordingly, a dual-band matching circuit for 2.4 and 5.8 GHz is designed and verified according to this equation.

A. DUAL-BAND PIFA
Meandering stubs can produce resonances in certain bands [25] based on the conventional PIFA concept. An antenna based on meandering line for dual-band are proposed (Fig. 2). The originally proposed model comprises a co-planar feeding line directly connected to the metallic ground and a meandering parasitic stub connected to the main
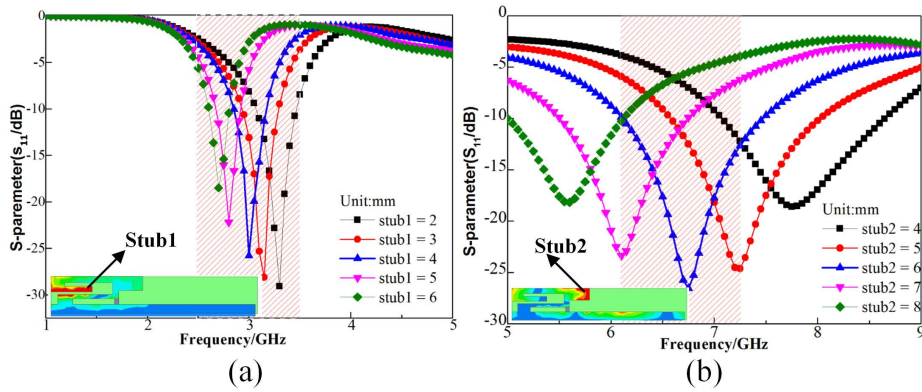
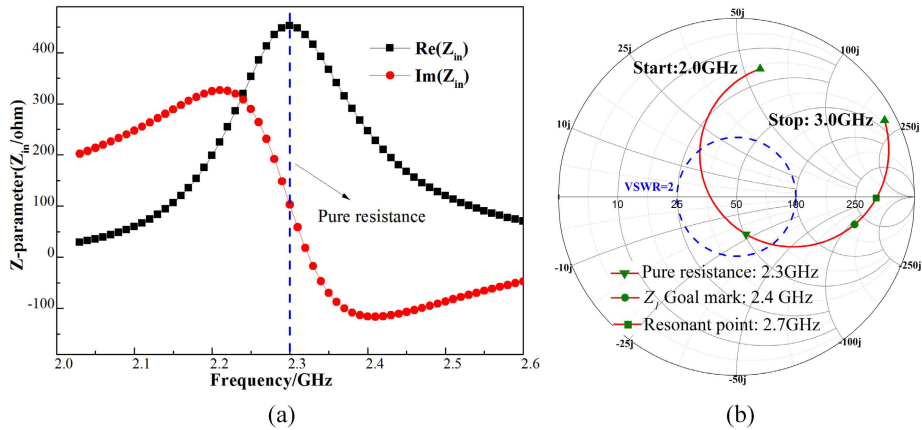**FIGURE 3.** S11 with variant lengths of (a) Stub1 and (b) Stub2.

FIGURE 4. The parameters Z of the original PIFA in the lower band of (a) Cartesian coordinate and (b) Smith chart.
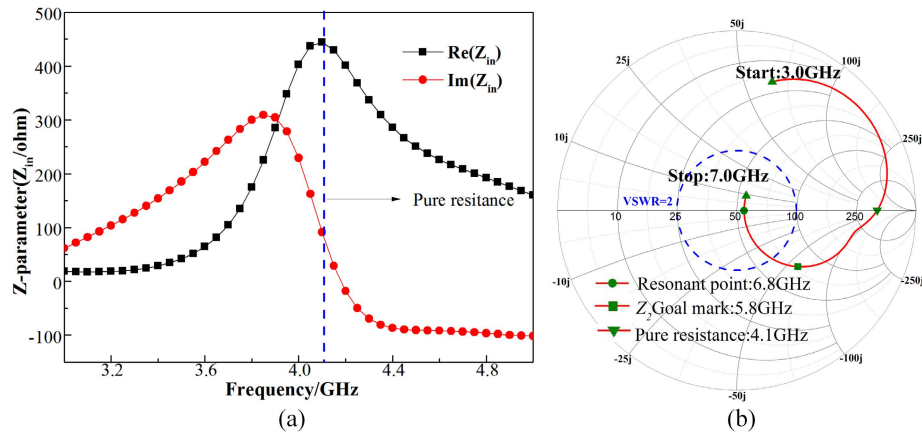

FIGURE 5. The parameters Z of the original PIFA in the higher band of (a) Cartesian coordinate and (b) Smith chart.

feeding line with a standard 50 Ohm matching impedance. Initially, it can already resonate respectively at 2.4 and 5.8 GHz [26]. However, a 25% size reduction is achieved to verify the dual-band matching scheme. Thus, the final values of the miniaturized antenna are listed in Table 1.

As depicted in Fig. 3, excited by a 2.4-GHz beam, heavy E field is focused on the stub 1 meaning a strong resonance

occurs at this position in the frequency. Likewise, when the exciting source is at 5.8 GHz, stub 2 takes on a critical significance in the resonance. Further comparisons between arm lengths of stub 1 and stub 2 are drawn, as presented in the Fig. 3. Notably, PIFA with current dimension will have higher resonant frequencies than 2.4 and 5.8 GHz though it may resonate at the frequencies of 2.4 and 5.8 GHz by extending
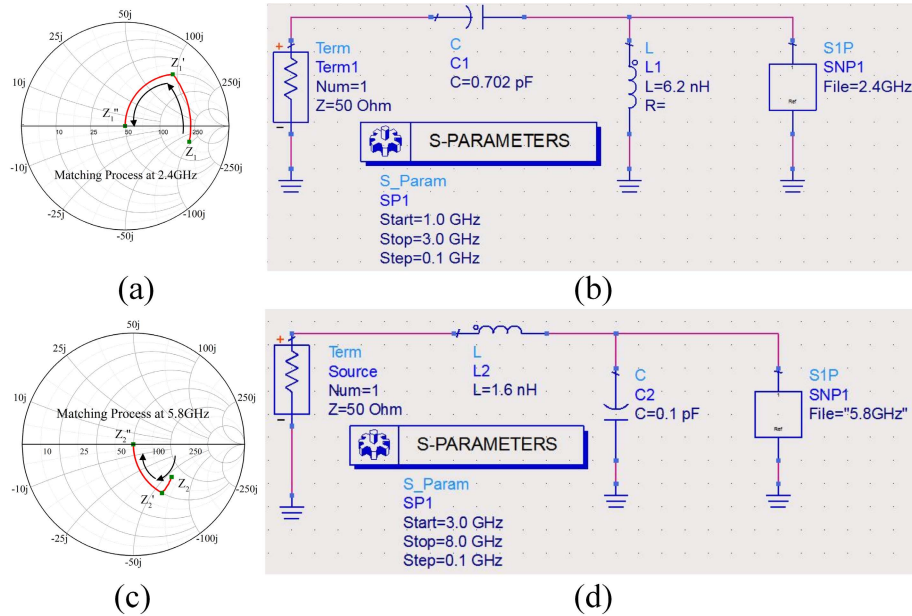
FIGURE 6. Matching process at (a) 2.4GHz and (b) 5.8GHz, matching circuit at (c) 2.4GHz and (d) 5.8GH.

TABLE 1. Dimensions of the raw antenna.

Parameters	w_1	w_2	w_3	w_4	w_5	w_6
Value(mm)	5	3.7	1.1	0.8	2.7	3.7
Parameters	L_1	L_2	L_3	L_4	L_5	H
Value(mm)	17.8	40	39.6	8	9	0.4

pure resistive status at 4.1 GHz, as depicted in Fig. 5(a), which can also be matched along its pure resistance horizontal axis in Fig. 5(b) of the Smith chart. As depicted in Figs. 4 and 5, the ideal resonance points at 2.4 and 5.8 GHz, represented by Z_1 and Z_2 in green, are not located in the center of the Smith chart outside the blue dashed coil. In fact, the general industry standard for matching designs is that it is useful for the desired resonance point to be located on the inside of the circle with VSWR (voltage standing wave ratio) equal to 2 outside of the blue dashed coil. Thus, the matching circuit can be designed based on the values extracted from the Smith chart.

the arm length of the stubs. Too long arm length will destroy the resonant structure of the PIFA.

B. PARAMETER EXTRACTION
Each RF load can be equivalent to a circuit composing of resistance, inductance and capacitance (RLC) [27]. Accordingly, the dual-band PIFA can be matched according to the above matching equation after the extraction of the equivalent parameters [17]. To clearly demonstrate the extraction of the equivalent parameters, the parameter Z, the input resistance and reactance of the proposed PIFA, are used to plot the extraction flow as shown below. In Figs. 4 and 5, the real and imaginary parts denote the input resistance and reactance of the proposed PIFA, respectively. In Cartesian coordinate of Fig. 4(a), the input impedance becomes a pure resistance approximately equivalent to 450 Ohm at the resonant frequency of 2.3 GHz, which is marked along the horizontal axis of the Smith chart, suggesting an LC resonance. Likewise, when the frequency ranges from 3 to 5 GHz, there is another

C. THE MATCHING FLOW
In general, two approaches can be adopted to design matching circuit aimed to allow the miniaturized antenna to operate at the desired 2.4 and 5.8 GHz, simultaneously [28], [29]. The first is to establish two compatible and independent circuits to steer Z_1 and Z_2 to the center of the Smith chart, respectively. Subsequently, the above two temporary circuits are cascaded and slightly modified to ensure that Z_1 and Z_2 are in the center of the Smith chart, simultaneously. Beginners can master the skill of circuit matching by the first method due to the independence of the above two circuits. The second is to choose one of the two points as the basic criterion, like 2.4 GHz as usual. Next, a temporary matching circuit is built, so Z_1 turns to the center of the Smith chart, and then another 5.8 GHz matching circuit is designed based on the previous temporary circuit. Lastly, the ultimate matching circuit can be completed and checked by modifications. It is not recommended to conduct the second way to design the matching circuit for dual-band antenna. There are an excessive number
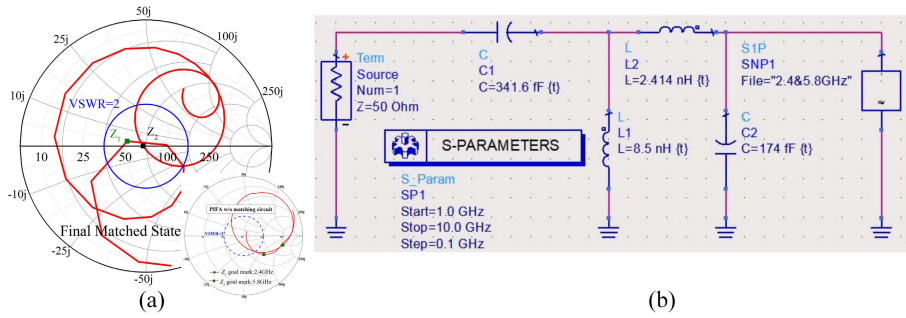
(a)   (b)

FIGURE 7. (a) Final state of smith chart, (b) final matched circuit.
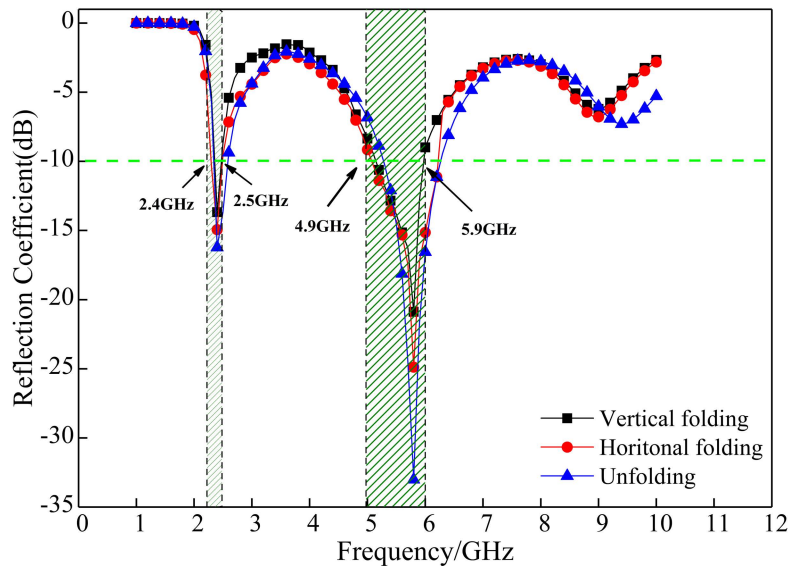

FIGURE 8. Reflection coefficients of PIFA with matched circuit.
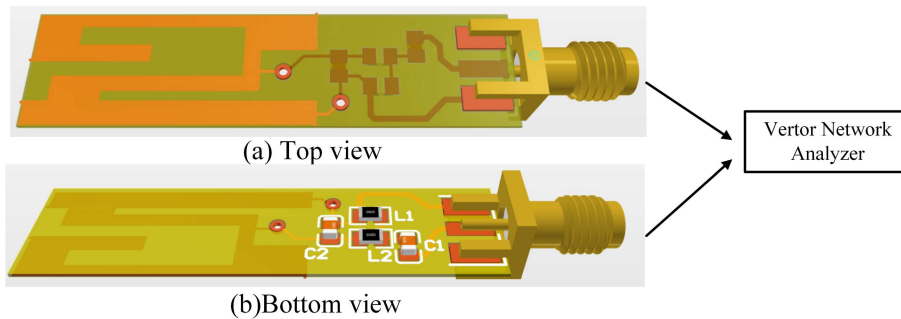

FIGURE 9. (a) Top view of integrated antenna. (b) Bottom view of integrated antenna.

of elements uncontrolled as slight modifications of elements in high band can significantly affect the elements in low band, thus destroying the previous design. However, two of the above approaches cannot achieve a perfect match until some optimization is performed. For convenience, a matching circuit will be built and analyzed in this study with the first approach as an example.

Z_1 (2.4 GHz) and Z_2 (5.8 GHz) are defined as the targeted points. The high frequency theory highlights the series capacitors and parallel inductors will affect the resonance result in the relatively high frequency band, while the series inductors and parallel capacitors will play a vital role in shifting resonant frequency in the relatively low band. Hence, Fig. 6(a) illustrates the process of designing a matching circuit for Z_1 (2.4GHz) first. Based on current point Z_1 in the Smith chart, its equivalent impedance Z of 175-94.4j Ohm can be obtained. The process of selecting elements in the Smith chart is illustrated in Fig. 6(b) in accordance with the
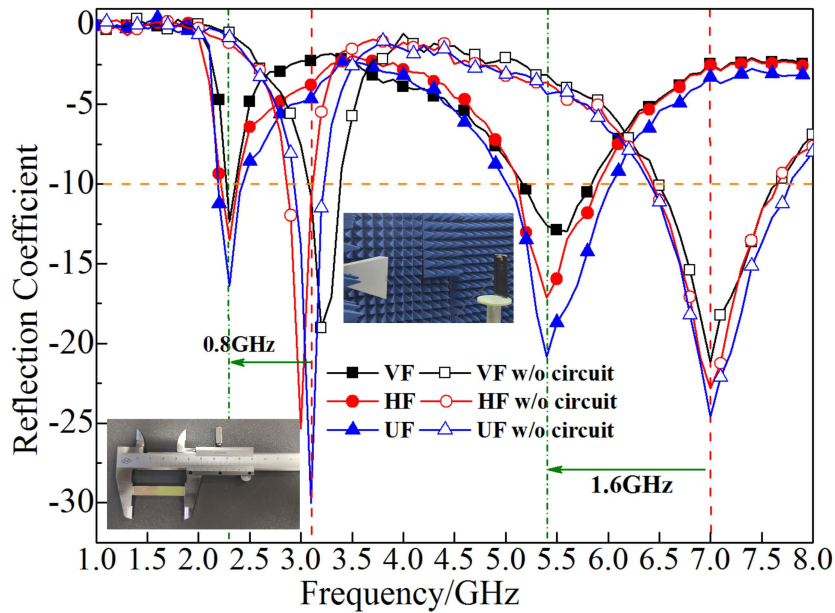
FIGURE 10. S11 of raw and matched miniaturized antenna in anechoic chamber.
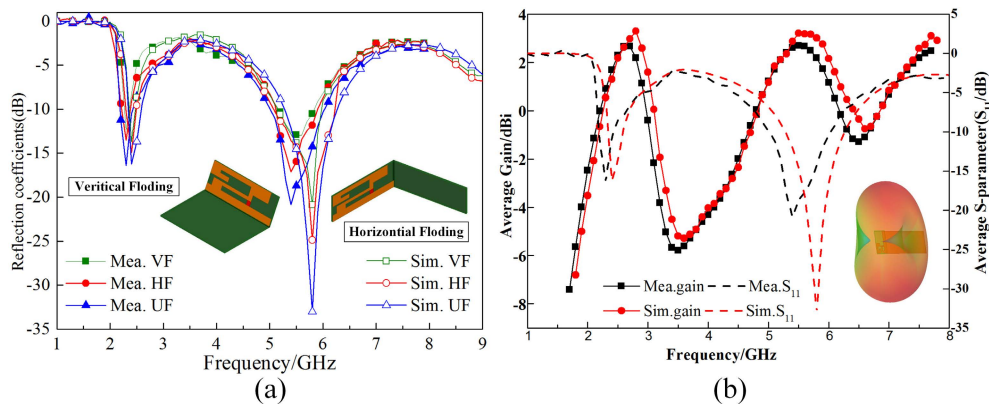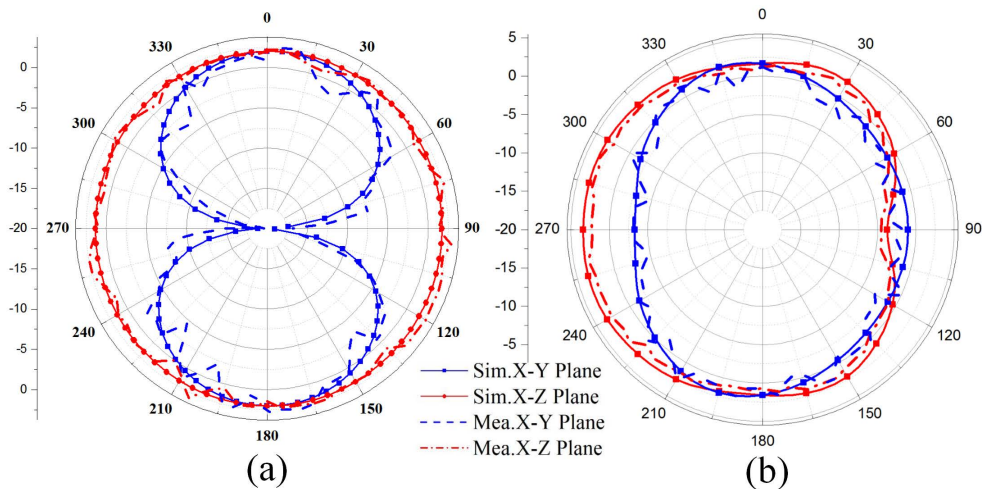

FIGURE 11. (a) S11 of simulation and measurement. (b) Gain of simulation and measurement.

high frequency principle concluded previously. There will be a series capacitor of 0.702 pF and a parallel inductor of 6.2 nH to steer the operating state from Z_1 to the center of the Smith chart. A similar approach of 2.4 GHz can be adopted to address the case of 5.8 GHz with parameter Z of 78.19-58.58j Ohm Accordingly, the matching process can be seen in Fig. 6(c) and another portion of the high frequency circuit can be obtained as shown in Fig. 6(d). So, in high frequency status, the initial values for matching circuit can be obtained as parallel capacitor of 0.1 fF and series inductor of 1.6 nH, respectively.

Lastly, the direct cascading of the above two temporary matching circuits allows the final matching stage, the F-type matching circuit, according to the principle of the previous radiating frequency circuit. Although Z_1 and Z_2 located in a circle with VSWR equals to 2 already met the requirements of manufacture industry criterion, some important optimizations

are always necessary to obtain more promising results. With the help of the software ADS, whose intrinsic function of tuning can optimize the respective component affecting the resonance results, the final matched circuit is likely to be determined, as depicted in Fig. 10, where $C_1 = 0.341$ pF, $L_1 = 85$ nH, $C_2 = 0.174$ pF, $L_2 = 2.414$ nH in principle. In addition, the final result in the Smith chart and the reflection coefficient of matched miniaturized antenna in unfolding, horizontal and vertical folding status are obtained in Figs. 7 and 8, respectively.

Compared with the simulated result in Fig. 3, Fig. 8 depicts the significant difference between raw and final antenna at 2.4 and 5.8 GHz after cascading a matching circuit. The reflection coefficient at 2.4 GHz is slightly stronger than that at 5.8 GHz in previous simulations. However, it is opposite in Fig. 8 since Z_2 is just located at the center, leading to a perfect LC resonance. The reflection coefficients of matched

FIGURE 12. Radiation patterns of simulation and measurement at (a) 2.4GHz and (b) 5.8GHz.

miniaturized antenna above suggest that the antenna exhibits a strong resonance of less than −10 dB at 2.4 and 5.8 GHz when the ground is unfolding, while vertical and horizontal folding has approximately the same S11 as unfold in the low band, whereas slight attenuation in the high band still meets the industry criterion. However, it makes no sense to conduct more optimization getting the most desired resonance points since it will cost much time for this eligible design. Furthermore, there are no certain components in the manufacturing industry with the same parameters as those in the simulation. The customized electronic components may lead to the high performance of the prototypes.

III. FABRICATION AND MEASUREMENT

The proposed miniaturized antenna with the designed matched circuit is developed on a FR4 substrate and examined by a VNA (Short for Vector Network Analyzer) with anechoic material plates surrounded as shown in Fig. 9 and Fig. 10, respectively.

In contrast to the raw antenna, the matched circuit can shift the targeted point from high band to relative lower ones, which are examined and plotted in Fig. 10 (VF, HF and UF short for vertical fold, horizontal fold and unfold, respectively, w/o short for without).

Fig. 11, shows a comparison between the simulated and examined reflection coefficients and gains, well consistent with each other. The following comparison results suggest that there is a slight offset in both bands due to the matching components. This is because there are certain specifications for the respective element in industry and fabrication.

The simulated and examined radiation patterns at 2.4 and 5.8 GHz are also examined and plotted in Fig. 12. The dual-band radiation patterns in measurement are well consistent with that in simulation. The jitter in angle and gain is negligible between simulation and measurement. As depicted in Fig. 12, the average gain at the desired frequencies can

be approximated at 3.7 dBi over such a small area. Furthermore, the directivity at 2.4 GHz is omnidirectional versus the 5.8 GHz who has some attenuation from 60 to 120 degree, which is only the rear of the mobile device and does not exert any effect during operation.

In addition, the vertical and horizontal folding does not have any effect on the primary part and ground of PIFA, and the radiation pattern will not significantly change.

IV. CONCLUSION

A matching theory for the miniaturization of dual-band component is proposed and discussed in this study, which is inspired by impedance matching for arbitrary frequency-dependent complex loads. A dual-band PIFA is miniaturized by an F-shaped circuit to meet the needs of folding and miniaturized devices in accordance with the proposed theory. Furthermore, a prototype was developed and examined in the experimental environment to verify the design. The results of reflection coefficient, radiation pattern and gain are well consistent with the simulated results. The matching circuit for miniaturization will be boosted in the future with the thriving of mini devices.

REFERENCES

[1] Y. Liu, Y.-J. Zhao, and Y. Zhou, "Lumped dual-frequency impedance transformers for frequency-dependent complex loads," *Prog. Electromagn. Res.*, vol. 126, pp. 121–138, 2012.

[2] Y. Liu, Y. Chen, and Y. J. Zhao, "Lumped triple-frequency impedance transformers," *Electron. Lett.*, vol. 48, no. 19, pp. 1193–1194, Oct. 2012.

[3] Y. Liu, Y. Zhao, S. Liu, Y. Zhou, and Y. Chen, "Multi-frequency impedance transformers for frequency-dependent complex loads," *IEEE Trans. Microw. Theory Techn.*, vol. 61, no. 9, pp. 3225–3235, Sep. 2013.

[4] A. Lehtovuori, R. Valkonen, and M. Valtonen, "Dual-band matching of arbitrary loads," *Microw. Opt. Technol. Lett.*, vol. 56, no. 12, pp. 2958–2966, 2014.

[5] X. Yang, Z. Ding, and Z. Zhang, "A complete flow of miniaturizing coil antennas based on matching circuit," *Electronics*, vol. 10, no. 10, p. 1159, May 2021.

[6] N. Nallam and S. Chatterjee, "Multi-band frequency transformations, matching networks and amplifiers," *IEEE Trans. Circuits Syst. I, Reg. Papers*, vol. 60, no. 6, pp. 1635–1647, Jun. 2013.

[7] J. H. Lu and Y.-S. Wang, "Internal uniplanar antenna for LTE/GSM/UMTS operation in a tablet computer," *IEEE Trans. Antennas Propag.*, vol. 61, no. 5, pp. 2841–2846, May 2013.

[8] Y. Chou, G. Lin, J. Chen, L. Chen, and M. Houng, "Design of GSM/LTE multiband application for mobile phone antennas," *Electron. Lett.*, vol. 51, no. 17, pp. 1304–1306, Aug. 2015.

[9] S.-C. Chen, M.-K. Wu, C.-W. Chiang, and M.-S. Lin, "3.5-GHz four-element MIMO antenna system for 5G laptops with a large screen-to-body ratio," *J. Electromagn. Waves Appl.*, vol. 34, no. 9, pp. 1195–1209, Jun. 2020.

[10] S. Y. A. Fatah, E. K. I. K. I. Hamad, W. Swelam, A. M. M. A. Allam, M. F. A. Sree, and H. A. Mohamed, "Design and implementation of UWB slot-loaded printed antenna for microwave and millimeter wave applications," *IEEE Access*, vol. 9, pp. 29555–29564, 2021.

[11] M. Czyz, J. Olencki, and A. Bekasiewicz, "A compact spline-enhanced monopole antenna for broadband/multi-band and beyond UWB applications," *AEU, Int. J. Electron. Commun.*, vol. 146, Mar. 2022, Art. no. 154111.

[12] K. N. Ketavath, D. Gopi, and S. Sandhya Rani, "*In-vitro* test of miniaturized CPW-fed implantable conformal patch antenna at ISM band for biomedical applications," *IEEE Access*, vol. 7, pp. 43547–43554, 2019.

[13] S. F. Jilani, M. O. Munoz, Q. H. Abbasi, and A. Alomainy, "Millimeter-wave liquid crystal polymer based conformal antenna array for 5G applications," *IEEE Antennas Wireless Propag. Lett.*, vol. 18, no. 1, pp. 84–88, Jan. 2019.

[14] S. Dehghani, S. Mirabbasi, and T. Johnson, "A 5.8-GHz bidirectional and reconfigurable RF energy harvesting circuit with rectifier and oscillator modes," *IEEE Solid-State Circuits Lett.*, vol. 1, no. 3, pp. 66–69, Mar. 2018.

[15] J. Sameer, M. Garza, J. Ruff, F. Espinal, D. Sessions, G. Huff, D. C. Lagoudas, E. A. P. Hernandez, and D. J. Hartl, "Self-foldable origami reflector antenna enabled by shape memory polymer actuation," *Smart Mater. Struct.*, vol. 29, no. 11, pp. 115011–115029, 2020.

[16] C.-T. Lee and S.-W. Su, "Tri-band, stand-alone, PIFA with parasitic, inverted-L plate and vertical ground wall for WLAN applications," *Microw. Opt. Technol. Letts.*, vol. 53, no. 8, pp. 1797–1803, Aug. 2011.

[17] S. Subbaraj, M. Kanagasabai, G. N. A. Mohammed, Y. P. Selvam, S. Kingsly, and R. R. Y. Venkata, "Miniaturized quad-band coplanar-fed monopole antenna for tablet computers," *COMPEL, Int. J. Comput. Math. Electr. Electron. Eng.*, vol. 37, no. 3, pp. 1118–1130, May 2018.

[18] Y. Tsutsumi, H. Kanaya, and K. Yoshida, "Design and performance of an electrically small slot loop antenna with a miniaturized superconducting matching circuit," *IEEE Trans. Appl. Supercond.*, vol. 15, no. 2, pp. 1020–1023, Jun. 2005.

[19] E. A. Hajlaoui, "A new compact dual band printed monopole antenna using electromagnetic band gap structures," *Circuit World*, vol. 43, no. 2, pp. 56–62, May 2017.

[20] G.-P. Gao, C. Yang, B. Hu, R.-F. Zhang, and S.-F. Wang, "A wearable PIFA with an all-textile metasurface for 5 GHz WBAN applications," *IEEE Antennas Wireless Propag. Lett.*, vol. 18, no. 2, pp. 288–292, Feb. 2019.

[21] N.-W. Liu, L. Zhu, and W.-W. Choi, "A low-profile wide-bandwidth planar inverted-F antenna under dual resonances: Principle and design approach," *IEEE Trans. Antennas Propag.*, vol. 65, no. 10, pp. 5019–5025, Oct. 2017.

[22] R. Jian, Y. Chen, and T. Chen, "A low-profile wideband PIFA based on radiation of multiresonant modes," *IEEE Antennas Wireless Propag. Lett.*, vol. 19, no. 4, pp. 685–689, Apr. 2020.

[23] M. M. Potrebić and D. V. Tošić, "Microwave memristive components for smart RF front-end modules," *Mem-elements for Neuromorphic Circuits With Artificial Intelligence Applications*. New York, NY, USA: Academic, 2021, pp. 67–98.

[24] Y. M. Pan, P. F. Hu, X. Y. Zhang, and S. Y. Zheng, "A low-profile high-gain and wideband filtering antenna with metasurface," *IEEE Trans. Antennas Propag.*, vol. 64, no. 5, pp. 2010–2016, May 2016.

[25] P. Ciais, R. Staraj, G. Kossiavas, and C. Luxey, "Design of an internal quad-band antenna for mobile phones," *IEEE Microw. Wireless Compon. Lett.*, vol. 14, no. 4, pp. 148–150, Apr. 2004.

[26] P. Bartwal, A. K. Gautam, A. K. Singh, B. K. Kanaujia, and K. Rambabu, "Design of compact multi-band meander-line antenna for global positioning system/wireless local area network/worldwide interoperability for microwave access band applications in laptops/tablets," *IET Microw., Antennas Propag.*, vol. 10, no. 15, pp. 1618–1624, Dec. 2016.

[27] A. García-Lampérez and M. Salazar-Palma, "Single-band to multiband frequency transformation for multiband filters," *IEEE Trans. Microw. Theory Techn.*, vol. 59, no. 12, pp. 3048–3058, Dec. 2011.

[28] E. Arabi, K. A. Morris, and M. A. Beach, "Analytical formulas for the coverage of tunable matching networks for reconfigurable applications," *IEEE Trans. Microw. Theory Techn.*, vol. 65, no. 9, pp. 3211–3220, Sep. 2017.

[29] V. Freitas, J.-D. Arnould, and P. Ferrari, "General expression for tunable matching network efficiency in the case of complex impedances," *Microw. Opt. Technol. Lett.*, vol. 57, no. 5, pp. 1160–1166, May 2015.

DAOHENG ZHU received the B.E. degree in communication engineering from the Wuhan Institute of Technology, Wuhan, China, in 2016, and the M.E. degree in information and communication engineering from Guizhou University, Guiyang, China, in 2020. He is currently pursuing the D.E. degree in marine science and technology with the School of Electronics and Information Engineering, Guangdong Ocean University, Zhanjiang, China. His current research interests include electromagnetic field, electromagnetic wave technology, and marine communication systems.

DAIAN LU received the B.E. degree in communication engineering and the M.E. degree in information and communication engineering from Guizhou University, Guiyang, China, in 2015 and 2018, respectively. He is currently with China Communications Services Guizhou Company Ltd., Guizhou Branch, Guiyang. His current research interest includes the development and maintenance of electromagnetic communication systems.

XIAOKUN YANG received the B.E. degree in communication engineering from the Wuhan Institute of Technology, Wuhan, China, in 2016, and the M.E. degree in information and communication engineering from Guizhou University, Guiyang, China, in 2019, where he is currently pursuing the D.E. degree in electronic science and technology with the School of Big Data and Information Engineering. His current research interests include electromagnetic field, electromagnetic wave technology, and wireless communication.

ZHIQIANG LI received the Ph.D. degree from Sun Yat-sen University, Guangzhou, China, in 2005. He is currently a Professor with the School of Electronics and Information Engineering, Guangdong Ocean University, Zhanjiang, China. He is a member of the Marine Disaster Reduction Science and Technology Branch, Chinese Society of Oceanography, and an Expert of emergency management with the Guangdong Provincial Education Department. His current research interests include marine remote sensing technology and its application and coastal engineering and environment.

● ● ●